STEADY-STATE RELATIVE PERMEABILITY MEASUREMENTS AND INTERPRETATION WITH ACCOUNT FOR CAPILLARY EFFECTS

by

G.A. Virnovsky, *RF-Rogaland Research, Stavanger, Norway,*
Y. Guo, *IBM-EPAC, Stavanger, Norway,*
S.M. Skjæveland, *Rogaland University Centre, Stavanger, Norway*
P. Ingsøy, *Esso Norge A.S., Stavanger, Norway*

Abstract

A multirate steady-state technique to measure relative permeabilities is presented. The technique eliminates interpretation errors related to the capillary end effect. To determine relative permeabilities of the two phases, individual phase pressure drops across the core have to be measured or calculated. In order to make the individual phase pressure drops measurable, a modified construction of the inlet end piece is suggested. Capillary end effects taking place during core flooding experiments at steady-state conditions both at inlet and outlet ends are theoretically analysed and studied by simulations in 2D.

Introduction

The steady-state technique to measure relative permeabilities is widely applied in core analysis. The inaccuracies in the conventional steady-state method mainly result from the basic assumption that capillary pressure may be neglected. As demonstrated earlier [1], errors due to capillary effects in steady state relative permeabilities may be quite large, especially in the saturation regions close to residuals where capillary pressure is large. In these saturation regions the capillarity related errors are difficult to avoid even at relatively high total rates.

A new method to measure relative permeabilities at steady-state conditions with account for capillary effects has recently been reported [2]. One of the main features of the new method is that for a fixed fractional flow at the inlet, a number of steady state points are taken with various total rates. The sensitivity of the effluent measurements to total rate can be used to correct for the capillary effects. The formulas and the corresponding experimental scenario are derived from the full set of two-phase flow equations in 1D, including capillary term. In this paper we consider a new construction for the inlet end piece allowing for measurement of individual phase pressures and study the continuity of phase pressures across the boundaries and two-dimensional effects close to the inlet end of the core. Some of these effects are encountered in conventional steady-state core-flooding experiments, while some of them are only relevant if the new construction of the end piece is used.

Experimental scenario and interpretation formulae

As demonstrated in [2], the following interpretation formulas may be derived from the standard set of equations describing steady-state two-phase flow in 1D,

$$S(0) = \frac{d(\bar{S}u_t)}{du_t} \,. \tag{1}$$

$$\lambda_1 = \frac{F}{\frac{d\Delta p_1}{du_t}} \frac{L}{k}, \qquad \lambda_2 = \frac{(1-F)}{\frac{d\Delta p_2}{du_t}} \frac{L}{k} \,. \tag{2}$$

All the saturation-dependent quantities in the eqs. (2) are referred to the saturation at the inlet end, determined from eq. (1).

One of several possible experimental scenarios is: for a fixed fractional flow F at the inlet, a number of steady-state measurement points is taken for various total rates. The change in the measured average saturation in the core and individual phase pressure drops will then allow to calculate the saturation at the inlet and the relative permeabilities corresponding to this saturation. The difference between the individual phase pressure drops will give the corresponding capillary pressure. One may proceed by changing the fractional flow at the injection to a new value, etc. At this point, special precautions should be made to avoid hysteresis.

A test of this scenario against synthetic data from a one-dimensional simulator is presented in Figures 1 and 2. In this example two fractional flows at injection are used: 1% an 99% of water. At F=1% the total injection rate has been stepwise decreased from 2 cc/min down to 0.02 cc/min. At F=99% the total injection rate has been stepwise increased from 0.02 cc/min up to 2 cc/min. With a capillary pressure being positive at low water saturations and negative at high ones (see Figure 2), this sequence of steps gives monotonous increase of the saturation at each point in the core. The two families of points in Figures 1 and 2 therefore correspond to the two fractional flows at injection, and the points in each family represent different total rates.

Both relative permeabilities and capillary pressure are accurately recovered if the flow is 1D and measurements are accurate enough. If the same data, i.e. the total pressure drop and the individual phase rates, are interpreted in a conventional manner using the Darcy's law the relative permeabilities become inaccurate because of negligence of capillary forces. The inaccuracy decreases with increasing total rate, nevertheless even at the high rate, 2 cc/min, the error in the relative permeabilities still is noticeable .

Another possibility is to perform a set of complete steady-state tests at different total rates, calculating corresponding relative permeabilities from Darcy's equation, and average saturation in the core (e.g. from material balance). This will result in a family of relative permeability curves parametrically depending on the total rate. The sensitivity of the measured relative permeability and average saturation to total rate allows for corrections to be made. Since each pair of the relative permeabilities corresponds to a specific direction of saturation change there is no problem to account for hysteresis in this case.

In both cases measurement of individual phase pressure drops is required. A possibility is to measure phase pressures directly in porous medium using the technique of semi-permeable pads implanted in the porous medium described in ref. [3]. Though principally possible, the techniques available are complicated and expensive, which create problems in application of those techniques for routine measurements.

To avoid phase pressures measurement in the porous medium itself, pressures could be measured outside the core, e.g., in the tubings or in the grooves of the end piece. These measurements are much easier to accomplish technically, the only question is whether they are

the same as the phase pressures inside the core, *whether the phase pressures are continuous across the boundary of the porous medium.*

If the assumption holds that the flow is one-dimensional then the behaviour of phase pressures across the boundaries may be analysed theoretically [2]. The results of this analysis show that (1) the non-wetting phase pressure is continuous at the inlet; (2) the capillary pressure is constant at the outlet, so that the total pressure drop measured outside porous medium is equal to the pressure drop in the non-wetting phase plus a constant value corresponding to the capillary pressure at the outlet.

For a typical imbibition capillary pressure curve crossing the saturation axes ($P_c = 0$), both phase pressures are continuous at the outlet, since the capillary pressure at the outlet is zero. At the inlet boundary, the wetting phase pressure is discontinuous. In this case the pressure drop measured outside the core is equal to the pressure drop in the non-wetting phase. Since saturation at the inlet end is calculated from eq. (1) independently of pressure values, the capillary pressure at inlet may be estimated from a capillary pressure curve measured separately. Then both individual phase pressure drops will be known.

With the existing hardware, only the total pressure drop outside the core is measurable. An attempt to measure individual phase pressure drops outside the porous medium will generally give large errors because of discontinuities of phase pressures across the boundaries of porous medium. A numerical investigation of the flow in the vicinity of the inlet end of the core was therefore undertaken and is reported below.

Modified construction of the inlet end-piece

In order to make individual phase pressures measurable, the construction of the inlet end piece is modified. The two phases are completely separated outside porous medium. The wetting phase (water) is injected into the core through a strongly water-wet material, e.g., semi-permeable membrane. (For a mixed-wet core it would also be necessary to have an oil-wet material between the core and the oil groove of the end piece.) The semi-permeable membrane is meant to prevent the counter-current flow of the non-wetting phase at inlet so that the water groove is filled only with water.

The flow in the core with the two types of end piece is studied by numerical simulations.

Simulation of inlet end-effects

Simulation grids:

3 different grid systems have been used in the simulation. In the grid system 1 and 2, 60 x 4 grid blocks were used, as shown in Figure 3. The first 7 blocks in X-direction represent the injection tubings: Layer 1 (Kv=50000 D, Kv=0.001 D, ϕ=0.5) for oil injection, layer 3 (Kv=50000 D, Kv=0.001 D, ϕ=0.5) for water injection, while layer 2 and 4 are tight (Kv=Kh=0.001 D, ϕ=0.001). The capillary pressure at this region is zero, and the relative permeabilities are linear functions of water saturation. The grid system 3 is similar to the grid system 2, however, with a grid refinement to represent a sandwiched water and oil injection regions. Total number of blocks in Y-direction is 8.

Core and fluid data:

Core length:	18.8 cm
Core diameter (= core thickness):	1 cm (thin grid) and 3.4 cm (for thick grid)
Core porosity(ϕ)	22%
Oil permeability (K_O at S_{wi}):	485 mD

Fluid viscosity:	μ_o = 1.06 cp, μ_w = 1.30 cp
Relative permeability curves:	Corey type with $N_1=N_2$= 2.0, $K_{ro}(S_{wi})=K_{rw}(S_{or})$=1.0
Capillary pressure curves:	1 for water-wet rock, 1 for mixed-wet rock (Figure 2).

Boundary and initial condition:

- Constant pressure at the core outlet end
- Constant oil injection rate into layer 1 (block No.(1,1)). For grid system 3, oil is injected through layer 1 and 5.
- Constant water injection rate into layer 3 (block No.3,1)). For grid system 3, water is injected through layer 2 and 7.
- Total injection rate: Qt = 2.0 cc/min (high rate) and Qt = 0.2 cc/min (low rate)
- Water fraction: 10%

Simulation results and discussions

Simulation with grid system 1. Grid system 1 represents the fluid flow situation associated with a conventional inlet end-piece. The capillary pressure is (close to) zero at the core inlet. Only the high-rate case is reported here. The injection pressure of the phases in the tubings are very close to each other, while the water phase pressure rapidly changes across the core boundary, see Figure 4. The non-wetting phase (oil) is expelled from the core into the water tubing since the core is water-wet. It forms a thin oil-filled zone in the water tubing attached to the inlet face of the core, see Figure 6. This oil film creates high resistance to water inflow causing discontinuity of the water phase pressure. This type of inlet end-effect is further referred to as TYPE 1. It is believed that this phenomenon happens frequently in conventional steady-state coreflood experiment.

Simulation with grid system 2. Grid system 2 is used to simulate a special end-piece by use of semi-permeable membranes. In this case, water is injected into the core through a water-wet membrane. The total rate used is 2.0 cc/min. The membrane has high capillary pressure in order to prevent oil from the core to enter into the water tubing. The simulation results confirm that the water tubing is kept saturated with water. The phase pressures in this case are both continuous from the core to the oil and water tubings. Figure 5 shows the pressure profiles, and Figure 7 the water saturation profiles. Compared to Figures 4 and 6, the inlet end-effect has been reduced dramatically.

However, it can be observed that the water saturation at the core inlet face is non-uniform due to the separate injection of fluids. In the vicinity of water tubing, water saturation tends to be higher than that close to the oil tubing, and vice versa for the oil saturation, although the average water saturation almost does not change along the core. The water saturation for each layer is displayed in Figure 8. Because of this phenomenon the phase pressures measured in the tubings will no exactly correspond to the average saturation at the inlet. We refer this effect as the inlet end-effect TYPE 2. The effect is more pronounced for the viscous dominated flow because the capillary imbibition transverse to the core can reduce the effect.

Simulation with grid system 3. As the inlet end-effect TYPE 2 is dependent on the geometry of the contact area between the injection fluid and the rock, the sandwiched configuration is believed to give a more even saturation distribution, i.e. the inlet end-effect of TYPE 2 can be reduced. The simulation results do show a more uniform saturation distribution due to higher degree of capillary dominance in the crossection of the core.

Simulations with varying rates and core length. Additional simulations have been conducted based on the grid system 1 and 2, but with varying core length (5 cm) and injection rate (2.0 and 0.2 cc/min). From the simulated results, one can conclude that the non-uniform saturation due to the end-effect TYPE 2 can be reduced with reduced injection rate and reduced core length, i.e., with the capillary dominance enhanced. Figure 9 shows the capillary pressure obtained from the tubing measurement as compared to the input. A relatively good match is obtained for the cases with semi-permeable membranes. The error due to the transverse non-uniformity of the saturation is largest for the least capillary dominated flooding. Large errors are observed for the cases without membrane.

Simulations with a complete steady-state cycle. Figure 10 is a simulation of steady-state imbibition test with 6 fractions: 5%, 10%, 20%, 50%, 75% and 100% water injection. Low rate (0.2 cc/min) and large core length is used.

The tubing pressures were used to convert capillary pressure at the saturation equal to the average water saturation at the inlet face of the core. Since the water saturation is relatively uniform in this case, the measured pressure drop between the tubings does reproduce the capillary pressure curve, although with some noticeable error. It is also worth to note that the total pressure drop across the core approaches the measurement limit (a few mbar) for this case.

Conclusions

- An inlet end effect due to the counterflow behaviour can be observed. It is characterised by a water pressure discontinuity and a non-uniform water saturation at the core inlet.
- Phase pressure continuity can be obtained by the use of semi-permeable membranes which allow only water or oil to enter the core. Simulations show that this inlet end-effect can be removed. The phase pressures become continuous from the core into the tubing. This offers a way of measuring individual phase pressure in the core at the fluid injection tubing.
- A second inlet end-effect is observed which is related to the separate injection of fluids. The water saturation is not uniform at the core inlet, an effect that will give errors in phase pressure. The degree of non-uniformity depends on the capillary dominance at the injection face, which is related to the injection rate, core length, and the magnitude of capillary pressure.

Nomenclature

F-pre-fixed fractional flow at the inlet of the core

k - absolute permeability of 1D porous medium

Kv, Kh -vertical and horizontal components of absolute permeability of 2D porous medium

L -length of the core

p_i-phase pressure, i=1,2

$P_c(S)$ - capillary pressure

S - saturation

$\overline{S}$ - average saturation in the core, $\overline{S} = \frac{1}{L}\int_0^L S(x)dx$

u_t-total velocity

x-coordinate

t-time

λ_i -phase mobility i=1,2

ϕ - porosity

Acknowledgement

The financial and technical support from Esso Norge a.s. and EXXON Production Research, Houston is gratefully acknowledged.

References

1. Virnovsky, G., Guo, Y., Vatne, K.O.. and Braun E.M.: "Pseudo steady state technique for relative permeability measurement." Proc. of the International Symp. of the Soc. of Core Analysts. 1994. p.217-226.
2. Virnovsky, G., Guo, Y., Skjæveland S.M.: "Relative permeabilities and capillary pressure concurrently determined from steady-state experiments." Proc. of the 8-th European Symp. on IOR, 15-17 Nay 1995, Vienna, Austria, v.1, p.60-69.
3. Richardson, J.G., Kerver, J.A., Hafford, J.A., and Osoba, J.S.: "Laboratory Determination of Relative Permeability", Trans. AIME, **195** (1952) 187-196.

Figures

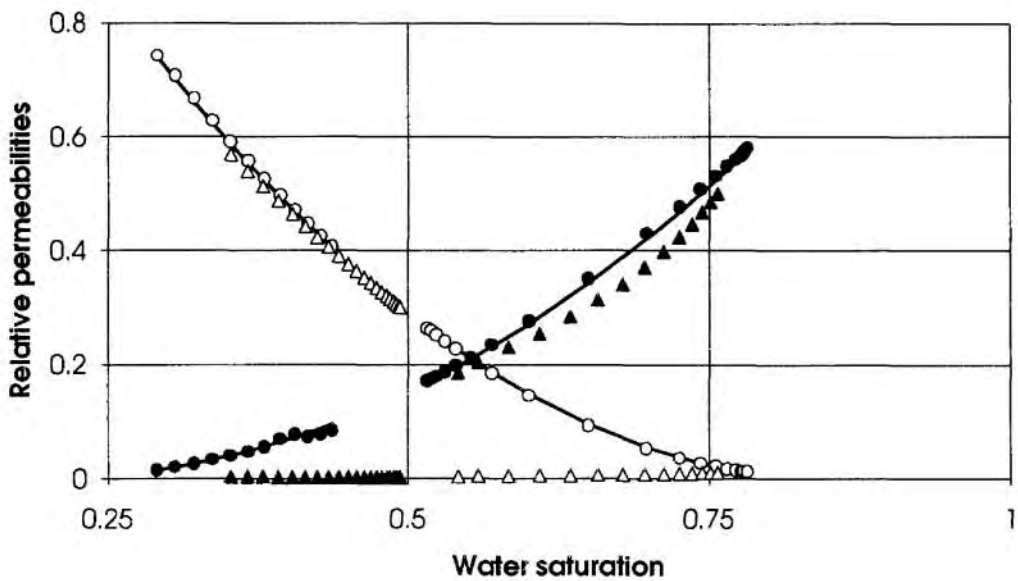

Figure 1. Relative permeabilities: calculated form the Darcy's law (triangles), corrected for capillary effects (circles) and the input functions (solid curves)

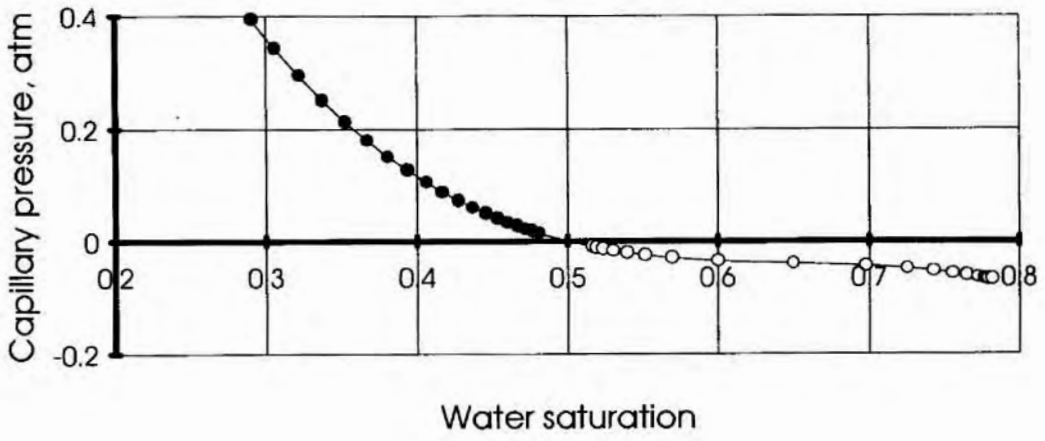

Figure 2. Calculated capillary pressure (circles), and the function from the simulator input. (solid line).

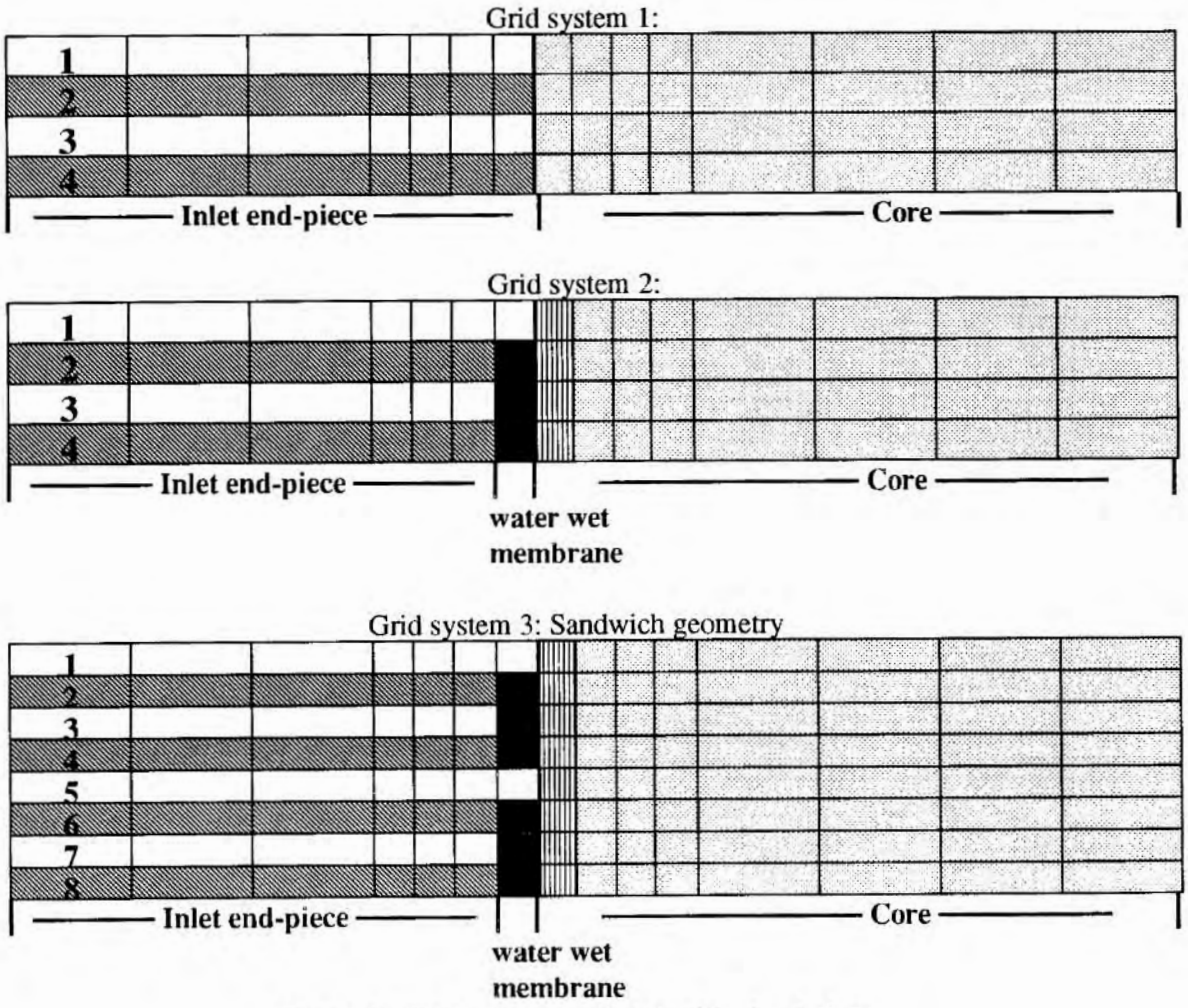

Figure 3 - Grid system used in the 2D-simulations

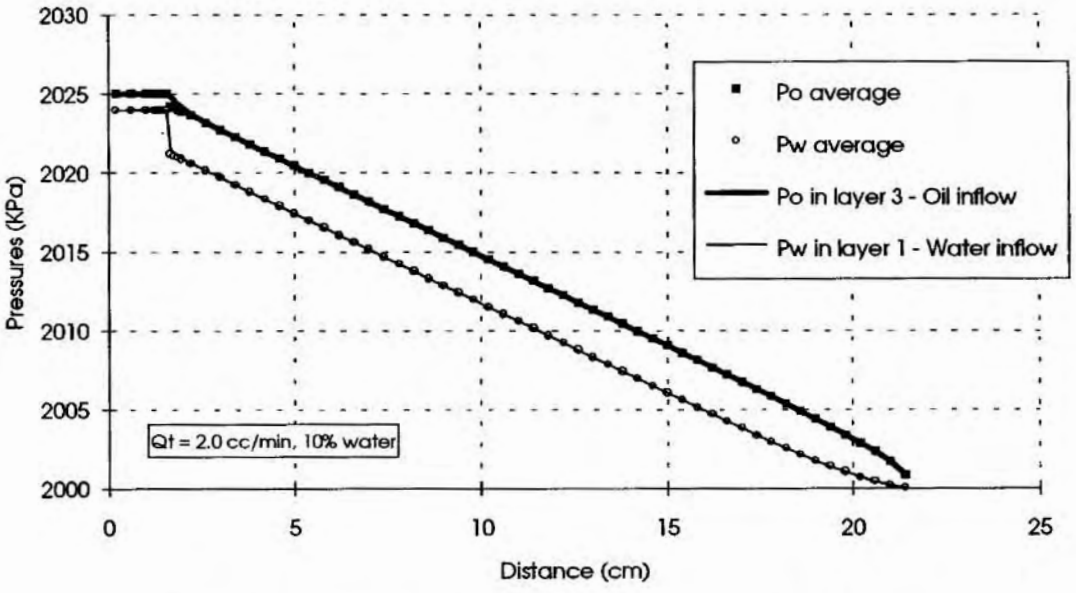

Figure 4 - Pressure distribution without membrane (Grid 1)

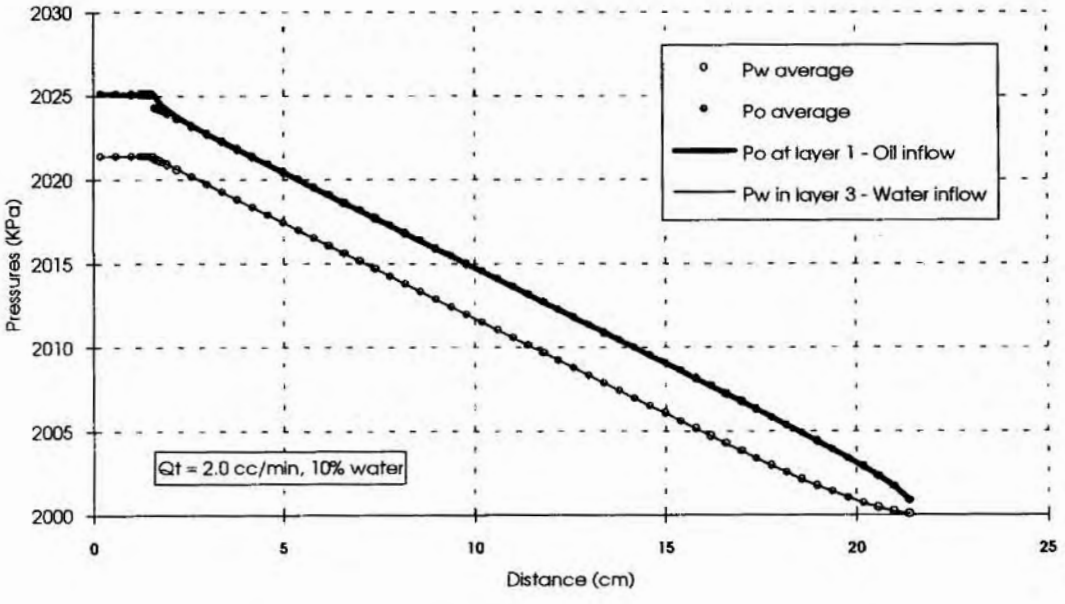

Figure 5 Pressure distribution with membrane (Grid 2)

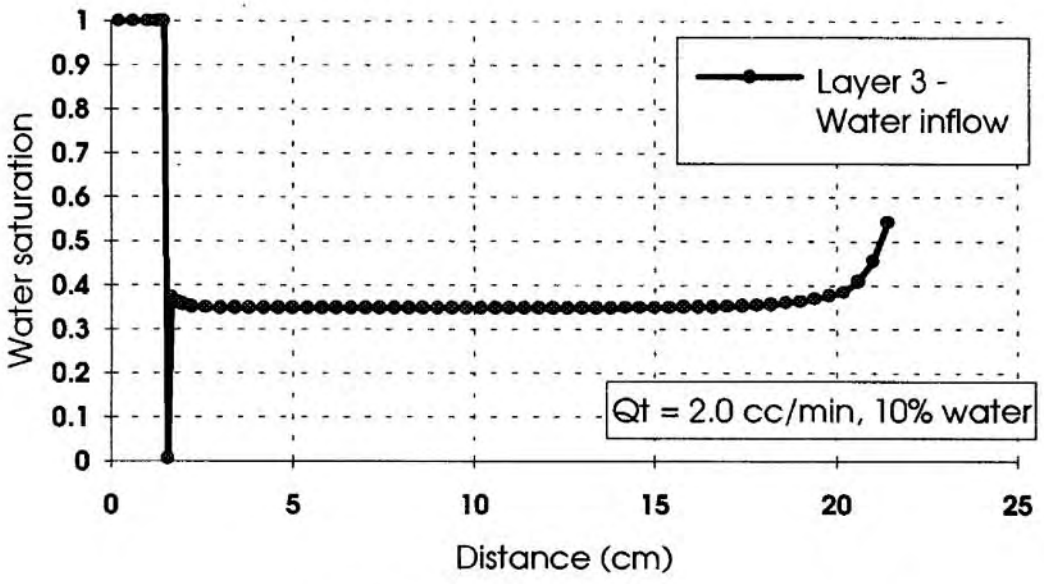

Figure 6. Saturation distribution without membrane (Grid 1)

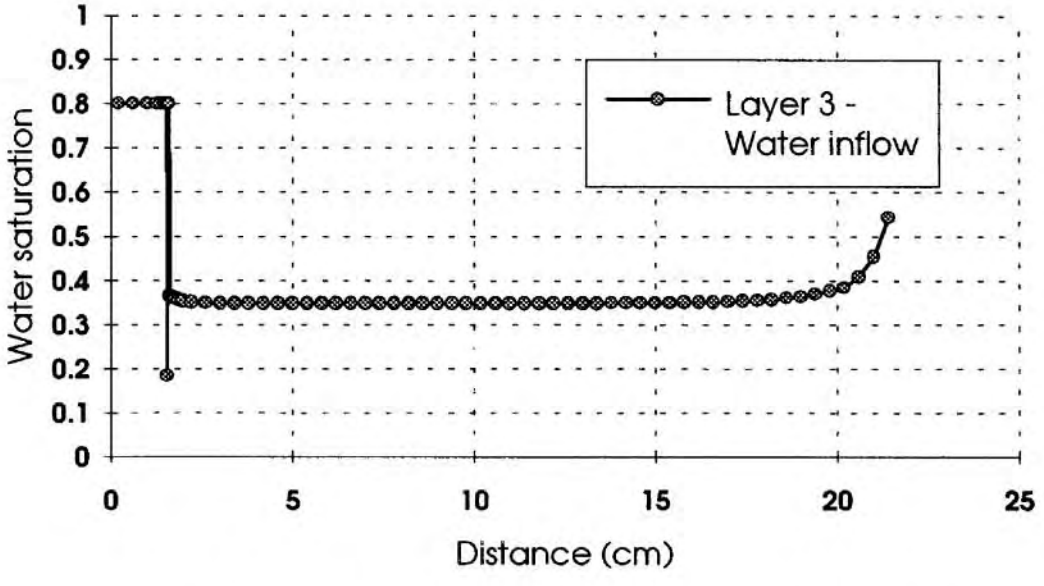

Figure 7 -Saturation distribution with membrane (Grid 2)

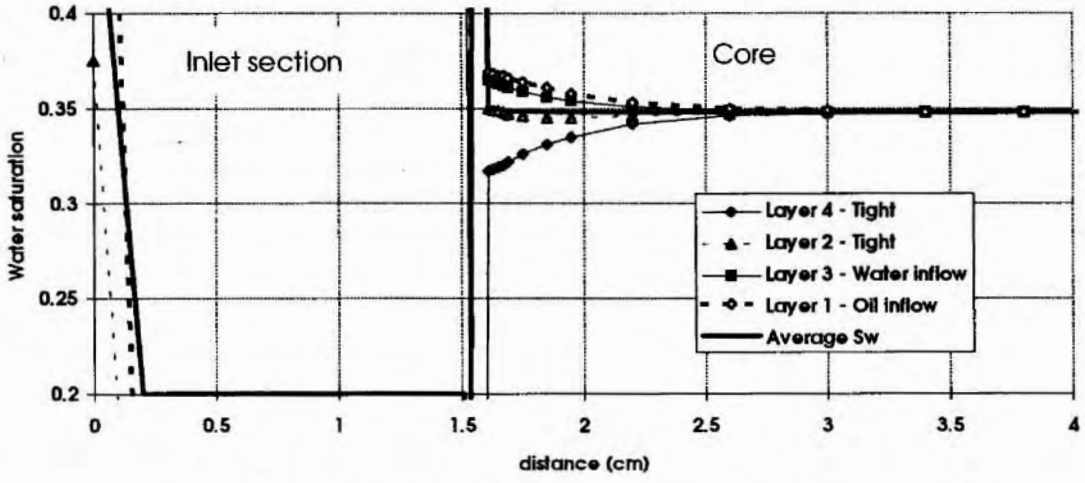

Figure 8 -Saturation distribution close to inlet with membrane (Grid 2)

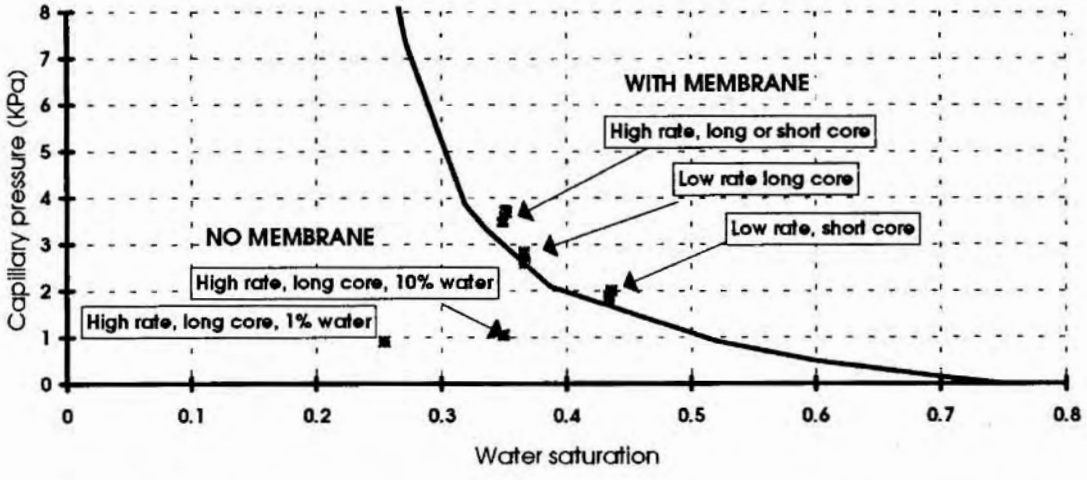

Figure 9. Capillary pressure recovered from tubing measurements at various rates and core lengths.

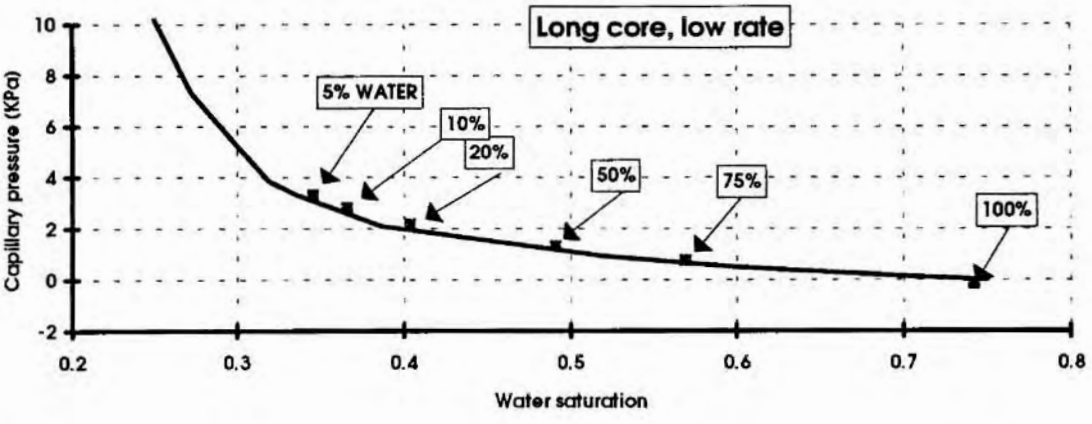

Figure 10. Capillary pressure recovered from tubing measurements at long core and low rate.